metry plane, where a is a dimension of the broad wall of the waveguide, the output signal decreases >30 times. Furthermore, by changing the position of the RS in the waveguide, the linear output signal dependence on the microwave power can be shifted to the desirable pulse power range. The VSWR was also obtained. It was determined that VSWR is <1.3 at $x = 0$, <1.2 at $x = 0.25a$ and <1.1 at $x = 0.46a$ over the entire X-band frequency range.

Table 1: RS testing results in anechoic chamber

U_s	P	U_{par}	L	W_p
V	kW	mV	cm	MW/m^2
0.039	0.030	–	246	0.088
0.077	0.059	–	175	0.17
0.23	0.17	5	96	0.51
1.9	1.4	20	32	4.3

The results of testing the RS in free space at several distances L between the horn antennas are presented in Table 1. By switching off the DC supply, the parasitic signal U_{par} induced by the external electromagnetic field can be detected. Its values are also shown in Table 1. With the help of the RS, a pulse power density up to 3.5MW/m^2 is detected. At that power density level, the parasitic signal is of the order of 1% of the useful signal.

Conclusion: An RS for high power short pulse measurement in the X-band was developed and fabricated. The proposed DC pulse supply allows an output signal from the RS of the order of a few tens of volts to be obtained without any amplification. Using the RS connected to the horn antenna, a pulse power density in free space of a few megawatts per metre squared was detected. It appears that the designed RS can be used at higher power levels that are practically limited by breakdown of the waveguide.

26 June 1995
Electronics Letters Online No: 19950916

M. Dagys, Ž. Kancleris, V. Orševskis and R. Simniškis (*Microwave Laboratory, Semiconductor Physics Institute, A. Goštauto 11, Vilnius 2600, Lithuania*)

References

1 BENFORD, J., and SWEGLE, J.: 'High-power microwaves' (Artech House, Boston-London, 1992)

2 DAGYS, M., KANCLERIS, Ž., SIMNIŠKIS, R., BÄCKSTRÖM, M., THIBBLIN, U., and WAHLGREN, B.: 'Microwave pulsed high power measurement in a free space making use of resistive sensors'. Proc. 23rd European Microwave Conf., 1993, pp. 506–507

3 DAGYS, M., KANCLERIS, Ž., SIMNIŠKIS, R., ORŠEVSKIJ, V., BÄCKSTRÖM, M., THIBBLIN, U., and WAHLGREN, B.: 'Measurement of high pulsed microwave power in free space', *IEEE Trans.*, 1995, **MTT-43**, (6), pp. 1379–1380

4 CONWELL, E.M.: 'High field transport in semiconductors' (Academic Press, N.Y., London, 1967)

Analogue VLSI 'integrate-and-fire' neuron with frequency adaptation

S.R. Schultz and M.A. Jabri

Indexing terms: Analogue circuits, Brain models, Neural chips

A silicon neuron with separated 'integrate' and 'fire' representations is presented. The neuron is simple and requires a modest number of transistors, but preserves a number of temporal characteristics of physiological neurons: temporal integration, passive conductance, after-hyperpolarisation, absolute refractory period, and frequency adaptation.

Introduction: Biological nervous systems have evolved to function in a dynamic environment. Therefore, temporal aspects must play an important role in neural computation. To build machines which function in the same dynamic environment, much can be learned from the rich temporal behaviour of biological neurons. A step in this direction is the construction in silicon of model neuronal elements which can compute in real time.

Mahowald and Douglas [1] reported a circuit which modelled specific ionic conductances to produce *in vitro* discharge patterns very similar to a neocortical pyramidal neuron. Sarpeshkar, Watts and Mead [2] presented a simple (eight transistor) neuron which incorporated a mechanism for the absolute refractory period of the neuron, but without adaptation of the firing rate for successive firings. Both of these circuits model the potential 'at the axon-hillock' of the neuron, i.e. where both the summated postsynaptic potentials and the 'sodium-spike' (action potential) are present in the membrane potential.

There is a strong motivation for representing separately the potential prior to the axonal trigger zone and the action-potential. This is needed for implementing physiologically-motivated plasticity (learning) mechanisms at the synapses of the neuron. Biophysical results indicate that the postsynaptic event required for associative learning, at least in the long-term potentiation (LTP) form of plasticity, depends on a 'consequence of dendritic depolarisation other than the elicitation of a sodium spike' [3]. A second motivation for a new neuronal circuit is the simple implementation of adaptation of the firing frequency, based on the assumption that this is important in neural dynamical behaviour [4]. We present a circuit that fulfils both criteria.

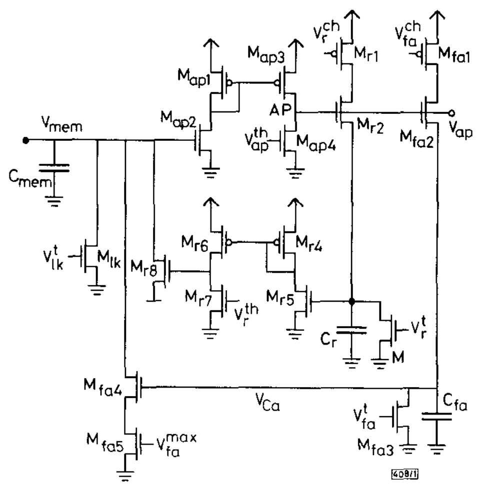

Fig. 1 *Circuit diagram for MOS 'integrate-and-fire' neuron*

Description of neuron circuit: The integrative function of the neuron (Fig. 1) occurs on the capacitor C_{mem}, which represents the 'membrane capacitance' of the neuron. Current is injected either by a synapse, or directly as might occur in an experimental situation, to produce the 'membrane potential' V_{mem}. Passive characteristics of the membrane are determined by the leakage transistor M_{lk}, which, although nonohmic in nature, is sufficient for the task.

Rather than mimicking the physiological workings of voltage-gated ion channels, their effect is considered functionally, so as to best take advantage of the medium of implementation. V_{mem} generates an exponentially increasing channel current in M_{ap2}. This current is compared at node AP with that generated by the (MOS subthreshold) action potential threshold, to produce an all-or-nothing action potential. The action potential injects a current determined by V_r^{ch} into C_r. When the voltage on C_r builds up enough to switch the comparator M_{r4-7}, the 'membrane potential' is pulled back down to the reset potential V_{ahp} through M_{r8}. V_{ahp} may range between small negative (after-hyperpolarising) voltages and the action potential threshold. This feedback loop plays a second role: for a period after the spike equivalent to the absolute refractory period of the neuron, while the comparator 'switch' remams on, no amount of injected current will induce the neuron to fire.

Frequency adaptation is implemented using an additional negative feedback loop around the firing mechanism. The action potential also injects current into C_{fa}, which together with M_{fa3} forms a leaky integrator. The voltage on the capacitor modulates another 'membrane conductance'. This conductance is comparable to the calcium-dependent potassium conductance, and the voltage on C_{fa} comparable to the intracellular calcium concentration of neurophysiology.

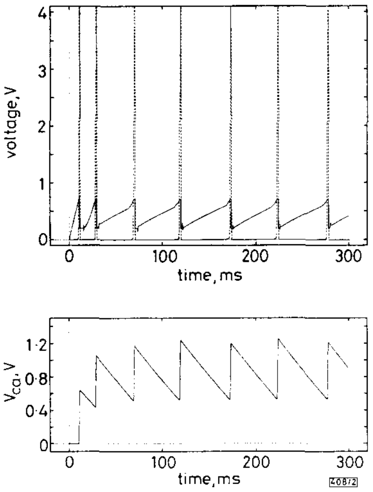

Fig. 2 *Response of 'membrane voltage', action potential, and 'intracellular calcium concentration' voltage to step of injected current of 110pA*

——— v_{mem}
– – – v_{ap}

Results of simulated experiments: Fig. 2 shows the superimposed 'membrane' and action potential for an applied step current: the *in vitro* situation. Also shown is the 'calcium concentration' voltage causing the frequency adaptation effect. Fig. 3*a* shows the adaptation of the current-to-frequency transduction curve with spiking activity. The results are qualitatively similar to those presented for a theoretical 'integrate-and-fire' neuron [4], and to data from physiological recordings [5].

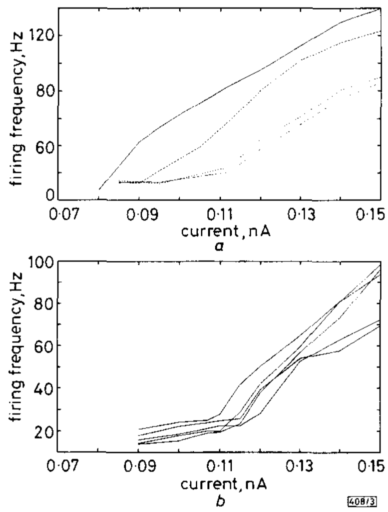

Fig. 3 *Firing frequency against injected current*

a Adaptation of firing frequency with successive spikes
b Saturated firing frequency curves for uniform distribution of parameters in 20mV band around values given in text
——— frequency-current relation without adaptation
– – – – instantaneous frequencies for each succeeding inter-spike interval, from top left to lower right

The parameter settings used to obtain these figures were: $V_{lk}{}^{t}$ = 0.60V, $V_{ap}{}^{th}$ = 0.70V, $V_{r}{}^{ch}$ = 4.35V, $V_{r}{}^{t}$ = 0.60V, $V_{r}{}^{th}$ = 0.50V, $V_{fa}{}^{ch}$ = 4.30V, $V_{fa}{}^{t}$ = 0.46V, $V_{fa}{}^{max}$ = 0.55V and V_{ahp} = 0.2V (SPICE parameters for the Orbit 1.2μm *n*well process were used). The system appeared to be functionally robust to variations in these parameters, as is illustrated in Fig. 3*b*. Owing to the 'all-or-nothing' nature of the action potential, mismatch of transistors will produce variation in the temporal characteristics rather than failure.

Conclusions: The neuronal circuit proposed is simple but preserves many of the essential temporal characteristics of biological neurons. It will provide a suitable element for studying dynamical issues in neural networks, such as rhythmic activity. Owing to the representation of the 'membrane voltage' just prior to the axon-hillock, it also prompts research into silicon 'plasticity' mechanisms capable of associative learning.

Acknowledgments: The authors wish to thank B. Flower for helpful suggestions and comments on an earlier draft of this Letter.

22 May 1995
Electronics Letters Online No: 19950932

S.R. Schultz and M.A. Jabri (*Department of Electrical Engineering, University of Sydney, NSW 2006, Australia*)

References

1 MAHOWALD, M., and DOUGLAS, R.: 'A silicon neuron', *Nature*, 1991, **354**, pp. 515–518
2 SARPESHKAR, R., WATTS, L., and MEAD, C.: 'Refractory neuron circuits'. CNS Technical Report No. CNS-TR-92-08, California Institute of Technology, Pasadena, California, 1992
3 KELSO, S.R., GANONG, A.H., and BROWN, T.H.: 'Hebbian synapses in hippocampus', *Proc. Natl. Acad. Sci. USA*, 1986, **83**, pp. 5326–5330
4 TREVES, A.: 'Mean-field analysis of neuronal spike dynamics', *Network*, 1993, **4**, pp. 259–284
5 KANDEL, E.R., SCHWARTZ, J.H., and JESSEL, T.M.: 'Principles of neural science' (Prentice-Hall Int., London, 1991)

Neural network restoration of images suffering space-variant distortion

S.W. Perry and Ling Guan

Indexing terms: Image reconstruction, Neural networks

A neural network algorithm for the restoration of images suffering space-variant distortion is introduced. Using multiple weighting matrices to represent space-variance, the algorithm provides high quality restorations in a computationally inexpensive fashion.

Introduction: Images recorded in many practical applications suffer space-variant distortions. It is well known that correction of such distortions is very difficult. The techniques available are either extremely computationally intensive (space-domain processing) and/or sensitive to the conditions of the distortion (space-invariant approximation).

We present a neural computing algorithm for restoring images degraded by space-variant distortion. Experimental results show that the proposed algorithm is able to provide high quality restorations efficiently.

Restoration model: Considering an $M \times M$ input image, in most cases the image degradation model is a linear distortion described by the equation [1, 2]

$$\mathbf{g} = \mathbf{H}\mathbf{f} + \mathbf{n} \qquad (1)$$

where **f** and **g** are lexicographically organised original and degraded image vectors, respectively, of size $M^2 \times 1$, **H** is a matrix distortion operator and **n** is an additive noise vector. This model is used here to describe images degraded by a space-variant distortion. We consider a simple form of space-variant distortion. The